Magnetostatic effects in giant magnetoresistive spin-valve devices

R. W. Cross[a] and Young K. Kim
Quantum Peripherals Colorado Inc., Louisville, Colorado 80028-8188

J. O. Oti and S. E. Russek
Electromagnetic Technology Division, National Institute of Standards and Technology, Boulder, Colorado 80303

(Received 7 June 1996; accepted for publication 9 August 1996)

We report on magnetotransport measurements of spin valve films that have been fabricated into rectangular stripes with Au current leads. The spin valve films consisted of two magnetic NiFe layers separated by a nonmagnetic Cu layer. The top NiFe layer was magnetically pinned by a FeMn layer with an effective pinning field of 12 kA/m (150 Oe). After device fabrication, the transport properties changed dramatically as the stripe-height of the device was decreased below 1 μm. Internal demagnetizing fields and magnetostatic interactions between the magnetic layers dominated the magnetic response. These interactions change the biasing point and the linearity, and cause a decrease in sensitivity to field changes. We have developed a simple single-domain rotation model that includes magnetostatic, anisotropy, and exchange interactions to describe the magnetic behavior, from which we calculate the transport response. © *1996 American Institute of Physics.* [S0003-6951(96)02943-9]

The primary focus of this work was to study spin valve devices as the height of the sensor was reduced below 1 μm. Most of the data reported on spin valves is for unpatterned films, which may have very different properties from device-level measurements.[6] We found that the most important interactions for small devices were magnetostatic, both internal demagnetizing fields and interlayer interactions between the magnetic layers. To better understand the results, we have developed a simple single-domain rotation model to describe the magnetic behavior of the spin valve devices. The calculation uses a Stoner–Wohlfarth model[7] for each layer and includes magnetostatic, anisotropy, exchange, pinning, and external field interactions.[8]

The spin-valve films were sputtered onto Al_2O_3-coated silicon wafers and then patterned using a wet-etch process into rectangular stripes with Au current leads for transport measurements, as shown in Fig. 1(a). The stripe-height (along x) varied from 16 to 0.5 μm while maintaining an aspect ratio of stripe height to length of 1–10 [Fig. 1(a) is not drawn to scale]. For the devices used in this study, the track width was set equal to the stripe height so that the active area was square. The track width defined by the current leads varied from 16 to 0.5 μm. The films consisted of a free layer of NiFe (7.5 nm), a spacer layer of Cu (3 nm), a pinned layer of NiFe (7.5 nm), a pinning layer of FeMn (10 nm), and a capping layer of Ta (5 nm). The pinning was accomplished by exchange coupling between the $Ni_{80}Fe_{20}$ to the antiferromagnetic $Fe_{50}Mn_{50}$ layer, which typically produces an effective pinning field of 12 kA/m (150 Oe). We did not add Co to the interfaces between the NiFe and Cu (which tends to increase the GMR by a factor of 2 or more),[9] in order to keep the system simple for modeling purposes. The easy axis was induced along the z-axis in the free layer by depositing the layer in a magnetic field.

Devices were fabricated with the pinning field aligned perpendicular to the stripe length, so, at zero field, the magnetic layers are 90° to each other (the free-layer magnetization prefers to align along the stripe length). This places the resistance at zero applied field in the middle of the linear region (bias point). The sheet-film GMR response shown in Fig. 1(b), for example, is biased near the center with high sensitivity and a large linear region. The pinning field keeps the upper NiFe layer from switching in fields up to 12 kA/m (150 Oe). The Cu thickness was 3 nm, just thin enough to produce a small ferromagnetic exchange interaction between the magnetic layers that slightly shifts the bias point.

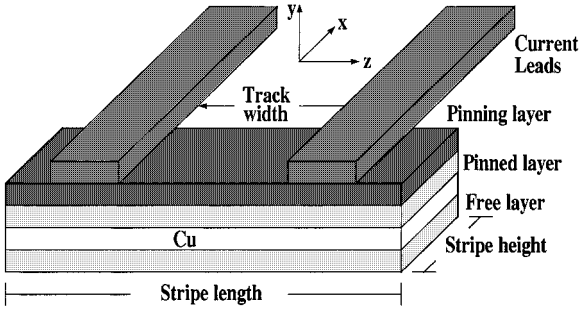

(a)

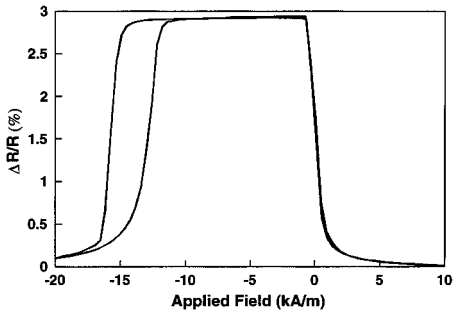

(b)

FIG. 1. (a) Schematic diagram of a spin-valve test device (not drawn to scale) and (b) a plot of $\Delta R/R$ for the sheet film response. The magnetic layers are NiFe (7.5 nm) with a 3-nm-thick Cu spacer and a pinning layer of FeMn (10 nm).

[a]Electronic mail: cross@QNTM.com

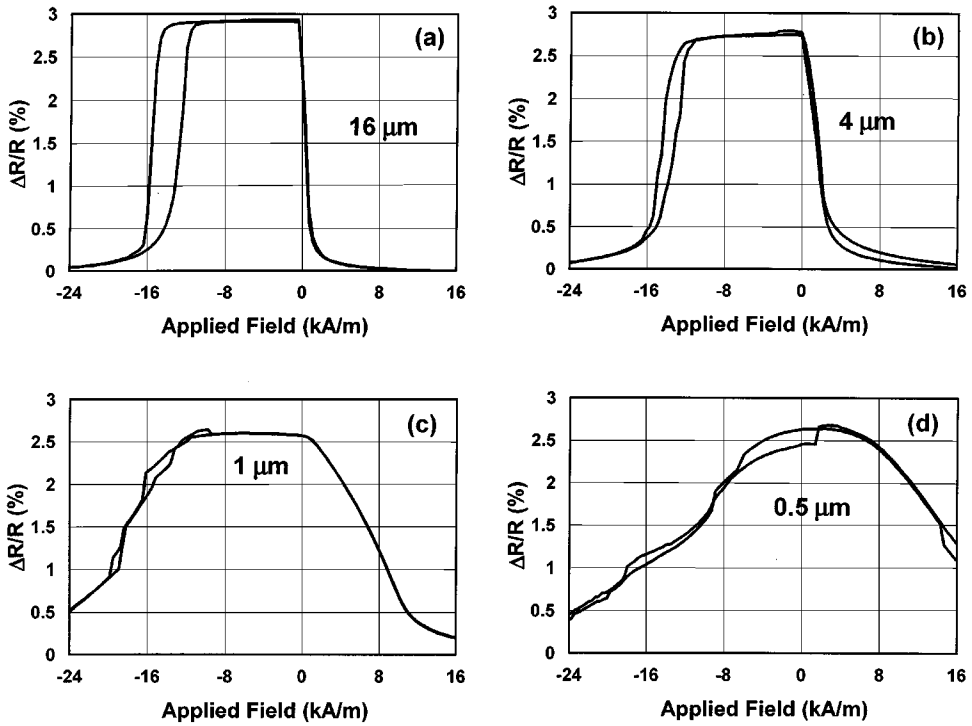

FIG. 2. Plots of GMR response as a function of device stripe height for (a) 16 μm, (b) 4 μm, (c) 1 μm, and (d) 0.5 μm. The stripe length is 10 times the stripe height.

The response of a device with a 16 μm stripe height, a 16 μm track width, and a Cu thickness of 3 nm is shown in Fig. 2(a). The center of the linear region has slightly shifted to positive fields due to magnetostatic interactions, but otherwise is very similar to the sheet film response shown in Fig. 1(b). The low-field portion of the curve has a large linear region with high sensitivity, which is very attractive for recording applications. Optimum biasing can be accomplished to some degree by using self-fields from the applied current and by controlling the exchange coupling between the magnetic layers.

As the device size decreases, however, the shape of the GMR curve becomes parabolic with a decrease in sensitivity from broadening of the response due to internal demagnetizing fields. With the large saturation magnetization value of NiFe (800 kA/m), small demagnetizing factors can cause fairly large magnetostatic fields. The response for different stripe heights is shown in Figs. 2(a)–2(d). The response of the 4 μm device begins to show a decrease in the slope of the linear region and slight rounding. For the 1 and the 0.5 μm devices shown in Figs. 2(c) and 2(d), the shape of the response is more nearly parabolic. Both internal and interlayer magnetostatic interactions between the NiFe layers become comparable to the pinning field. As the stripe height decreases, the transverse demagnetizing fields increase because of the constant film thickness. For example, the effective demagnetizing field at 16 μm is approximately 0.32 kA/m (4 Oe) and increases to over 4 kA/m (50 Oe) for the 1 μm device.

The bias points for the curves in Fig. 2(b) and 2(c) are nearly the same with the pinned layer still pinned along the x axis (90°), but now the free layer is locked at approximately $-90°$ due to the magnetostatic fields from the pinned layer. This alignment is assumed because the resistance is a maximum (and is similar to the sheet film's maximum resistance), corresponding to antiparallel alignment. The alignment is maintained over a range of stripe heights from 1 to 5 μm. We attempted to correct the bias of the 1 μm device using self-fields from large applied current densities, but were only able to produce small shifts up to 2×10^7 A/cm^2.

As the stripe height decreases, the magnetostatic fields between the layers and the internal demagnetizing fields become comparable to the pinning field. (The interlayer magnetostatic fields scale with the internal demagnetizing fields.) For the extreme case shown in Fig. 2(d), the free layer and the pinned layer rotate into antiparallel alignment at zero field, producing a parabolic response (much like what is seen in a multilayer). The magnitude of $\Delta R/R$ remains nearly the same for all of the devices [Figs. 2(c) and 2(d) are not completely saturated; otherwise the values are similar]. This indicates that at least the material properties involved with the transport have not severely degraded with device fabrication, although the pinning field may have degraded, which will be discussed later. To better understand the magnetic behavior, we have developed a simple model that treats the magnetization in each layer as a single domain.[11,12]

The magnetic layers of a spin valve are treated as single-domain films, and their magnetic behaviors are modeled using the Stoner–Wohlfarth coherent rotation model[7] of the magnetization reversal of a uniformly magnetized ellipsoid. We extended the model developed in Ref. 8 to include a transverse uniaxial anisotropy field in the pinned layer. The free energy density of the *pinned* magnetic layer is given by the expression[8]

$$W=\tfrac{1}{2}M_s^2(N_x\alpha^2+N_y\beta^2+N_z\gamma^2)-|H_0+H_p+H_m(M_{s'})|M_s(l\alpha+m\beta+n\gamma)+\tfrac{1}{2}H_kM_s(1-\alpha^2)+\tfrac{1}{2}H_{k\text{-pin}}M_s(1-\gamma^2), \quad (1)$$

where H_0 is the externally applied field; H_p is the pinning field; $H_m(M_s')$ is the interlayer magnetostatic interaction field; α, β, and γ are the direction cosines of the magnetization of the film M_s; l, m and n are the direction cosines of the total field $H_0+H_p+H_m(M_s')$; and N_x, N_y, and $N_z(N_x+N_y+N_z=1)$ are the demagnetizing factors along the three principal axes of the film. The easy-axis anisotropy field along the longitudinal direction H_k is induced by sputtering in a magnetic field.

Surface charges on the boundaries of the rectangular films are the field sources used in calculating H_m. Other fields, such as the self-field due to current flowing through the device, and possible effective exchange interaction field between the magnetic layers, may be included in the applied-field term in Eq. (1). We have also included a *transverse* uniaxial anisotropy term $H_{k\text{-pin}}$ in the energy expression for the pinned layer to account for the observed hysteresis at high fields when the layer unpins and rotates to align along the applied field. The general form is given in the last term in Eq. (1).

An expression similar to (1) follows for the energy density of the free layer by interchanging the roles of M_s and M_s', and omitting the pinning field term and the transverse anisotropy term. For the free layer, H_m is the interlayer magnetostatic interaction field acting on it due to the magnetization of the pinned layer. More of these issues are described in detail in Ref. 8. The change in the resistance is proportional to $\Delta R=1-\cos\theta$, where θ is the angle between the magnetization vectors of the layers. The proportionality constant is found by matching the fit to the experimental data.

Plots of the calculated response as a function of device size are shown in Fig. 3. The parameters for the calculation were found by fitting the 16 μm stripe-height device first and then using the same parameters to fit all of the other devices. The parameters used in the fits are $H_p=12$ kA/m (150 Oe), $H_{k\text{-pin}}=4$ kA/m (50 Oe), $H_k=0.64$ kA/m, NiFe thickness $=7.5$ nm, and $M_s=800$ kA/m. The exchange field measured in the films for a Cu thickness of 3 nm was small and was neglected in the calculation. We can derive various conclusions from the model fits. (1) The internal demagnetizing fields rotate the layers toward the stripe length. This energy term becomes larger than the pinning interaction for devices smaller than 1 μm and causes a decrease in sensitivity (decreases the slope). (2) The interlayer magnetostatic energy terms favor antiparallel alignment. The interaction is the largest external contributor to the total energy of the free layer for devices $\leqslant 1$ μm. It is this interaction that shifts the bias point and in the extreme case produces the parabolic response for the very small devices. (3) To properly fit the 1 and 0.5 μm device curves, we found that the pinning field decreases with device size (this was not done for the curves shown in Fig. 3). The pinning field shifts the curve toward negative field and flattens the response more than is observed experimentally. The little shift observed in Fig. 2(d) suggests that the effective pinning field is very small for the 0.5 μm device. To properly fit the response, we used a pinning field of 0.8 kA/m. The reduction in pinning field is not totally unexpected considering the corrosive nature of the FeMn pinning layer. We expect that some corrosion occurs from the edges inward and becomes serious for the smaller devices. The fact that the 0.5 μm device exhibits GMR with very little pinning is important because we find that magnetostatic coupling can be used to obtain antiparallel alignment and still realize the full $\Delta R/R$. If we calculate demagnetizing energy as a function of stripe height, we find that the demagnetizing energy grows larger than the pinning energy just below 1 μm and is inversely proportional to the stripe height. The arrows in the plots show the relative orientation of magnetization in each layer at the bias point. As the stripe height decreases, the magnetostatic fields rotate the magnetization from transverse bias toward antiparallel alignment.

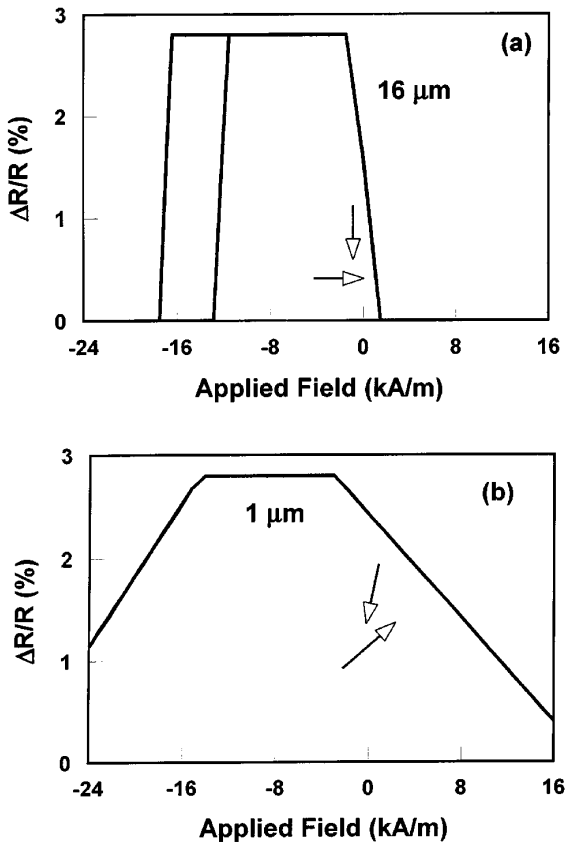

FIG. 3. Calculations of GMR response as a function of device stripe heights for (a) 16 μm and (b) 1 μm. The stripe length is 10 times the stripe height. The parameters used in the fits are $H_p=12kA/m$, $M_s=800$ kA/m, $H_{s\text{-pin}}=4$ kA/m, and $H_k=0.64$ kA/m. The magnetic layers are assumed to be identical with thicknesses of 7.5 nm. The arrows show the relative orientation of magnetization at the bias point; the top arrow represents the pinned layer and the bottom arrow represents the free layer.

[1] R. W. Cross, S. E. Russek, S. C. Sanders, M. R. Parker, J. A. Barnard, and S. A. Hossain, IEEE Trans. Magn. **30**, 3825 (1994).
[2] C. E. Johnson, J. Appl. Phys. **33**, 2515 (1962).
[3] J. O. Oti, R. W. Cross, S. E. Russek, and Y. K. Kim, J. Appl. Phys. **79**, 6386 (1996).
[4] D. E. Heim, R. E. Fontana, C. Tsang, V. S. Speriosu, B. A. Gurney, and M. L. Williams, IEEE Trans. Magn. **30**, 316 (1994).
[5] S. Middelhoek, *Ferromagnetic Domains in Thin Ni-Fe Films* (Drukkerij Wed. G. Van Soest, N. V., Amsterdam, 1961).
[6] R. W. Cross, J. O. Oti, S. E. Russek, T. Silva, and Y. K. Kim, IEEE Trans. Magn. **31**, 3358 (1995).